Ecotoxicology and Environmental Safety 211 (2021) 111942

Contents lists available at ScienceDirect

Ecotoxicology and Environmental Safety

journal homepage: www.elsevier.com/locate/ecoenv

Magnetite nanoparticles coated with citric acid are not phytotoxic and stimulate soybean and alfalfa growth

María Florencia Iannone [a,b,*], María Daniela Groppa [a,b], Myriam Sara Zawoznik [a], Diego Fernando Coral [c,1], Marcela Beatriz Fernández van Raap [c], María Patricia Benavides [a,b]

[a] Facultad de Farmacia y Bioquímica, Universidad de Buenos Aires, Junín 956, 1113 Buenos Aires, Argentina
[b] Instituto de Química y Fisicoquímica Biológicas (IQUIFIB-CONICET), Departamento de Química Biológica, Facultad de Farmacia y Bioquímica, Universidad de Buenos Aires, Junín 956, 1113 Buenos Aires, Argentina
[c] Instituto de Física de La Plata (IFLP, CONICET), Departamento de Física, Facultad de Ciencias Exactas, Universidad Nacional de La Plata, c.c. 67, 1900 La Plata, Argentina

ARTICLE INFO

Editor by Dr. Muhammad Zia-ur-Rehman

Keywords:
Alfalfa
Growth
Iron nanoparticles
Oxidative stress
Soybean
Translocation

ABSTRACT

In this work, the internalization and distribution of citric acid-coated magnetite nanoparticles (here, Fe_3O_4-NPs) in soybean and alfalfa tissues and their effects on plant growth were studied. Both legumes were germinated in pots containing an inert growing matrix (vermiculite) to which Hoagland solution without (control, C), with Fe_3O_4-NPs (50 and 100 mg iron L^{-1}, NP50 and NP100), or with the same amount of soluble iron supplied as Fe-EDTA (Fe50, Fe100) was added once before sowing. Then, plants were watered with the standard nutrient solution. The observation of superparamagnetic signals in root tissues at harvest (26 days after emergence) indicated Fe_3O_4-NPs uptake by both legumes. A weak superparamagnetic signal was also present in the stems and leaves of alfalfa plants. These findings suggest that Fe_3O_4-NPs are readily absorbed but not translocated (soybean) or scarcely translocated (alfalfa) from the roots to the shoots. The addition of both iron sources resulted in increased root weight; however, only the addition of Fe_3O_4-NPs resulted in significantly higher root surface; shoot weight also increased significantly. As a general trend, chlorophyll content enhanced in plants grown in vermiculite supplemented with extra iron at pre-sowing; the greatest increase was observed with NP50. The only antioxidant enzyme significantly affected by our treatments was catalase, whose activity increased in the roots and shoots of both species exposed to Fe_3O_4-NPs. However, no symptoms of oxidative stress, such as increased lipid peroxidation or reactive oxygen species accumulation, were evidenced in any of these legumes. Besides, no evidence of cell membrane damage or cell death was found. Our results suggest that citric acid-coated Fe_3O_4-NPs are not toxic to soybean and alfalfa; instead, they behave as plant growth stimulators.

1. Introduction

Nanotechnology has become a hotspot in research and development, and iron oxide nanoparticles (IO-NPs) have attracted particular attention because of their unique properties, which make them suitable for a wide range of applications in different fields such as biomedicine, pharmaceutical industry, environmental remediation, construction, electronics, and textile and automotive industry (Ali et al., 2016 and references therein). However, iron oxides with bare surfaces tend to agglomerate due to strong magnetic attraction among particles, high energy surface, and van der Waals forces (Xia et al., 2012). To avoid agglomeration, magnetic nanoparticles can be coated with organic or inorganic molecules, making them hydrophilic, biocompatible (Wu et al., 2008), and functionalized (Sheng-Nan et al., 2014).

De Sousa et al. (2013) reported that magnetite nanoparticles coated with citric acid improved nanoparticle suspension stability with little effect on the hydrodynamic radii; these nanoparticles have the advantage of combining electrostatic and steric stabilization and being biocompatible.

As most nanoparticles (NPs), IO-NPs may reach the soil as a result of

Abbreviations: DW, dry weight; FW, fresh weight; IO-NPs, iron oxide nanoparticles; ROS, reactive oxygen species; VSM, vibrating sample magnetometry.

* Correspondence to: Facultad de Farmacia y Bioquímica, Universidad de Buenos Aires, Junín 956, 1113 Buenos Aires, Argentina.
E-mail address: mfiannone@ffyb.uba.ar (M.F. Iannone).
[1] Present address: Departamento de Física, Universidad del Cauca, Popayán, Colombia.

https://doi.org/10.1016/j.ecoenv.2021.111942
Received 7 October 2020; Received in revised form 23 December 2020; Accepted 12 January 2021
Available online 19 January 2021

anthropogenic activity (Gladkova and Terekhova, 2013), and new nanoremediation approaches including those associated with wastewater treatments may be responsible for the release of significant amounts of IO-NPs in the environment (Attia and Elsheery, 2020; Sun, 2019). Once released into the agro-environment, several transformations facilitate their accumulation into the soil (Rajput et al., 2020). Subsequently, they can enter the plants by the roots; uptake depends on NPs properties, plant species, and environmental conditions (Chen, 2018). NPs may diffuse from the soil to the roots by several processes such as osmotic pressure and capillary action forces (Govea-Alcaide et al., 2016 and references therein). Furthermore, it was reported that NPs can enter into roots through the apoplastic or symplastic route (Rico et al., 2011; Tombuloglu et al., 2019a; Zhai et al., 2014).

Despite the presence in root tissue of biological barriers that may difficult NPs movement (cell wall, Casparian strip), some NPs were found to be translocated to the aerial parts and accumulate in cellular or subcellular compartments (Al-Amri et al., 2020 and references therein). It was reported that plants and NPs features play crucial roles in NPs translocation. For instance, Zhu et al. (2012) reported that Au-NPs could be stored in *Oryza sativa* shoots, but these NPs did not accumulate in the shoots of *Raphanus sativus* and *Cucurbita mixta.* Further investigation of NPs uptake and translocation by plants should be done, as there are still no conclusive results (Servin et al., 2015). It should be noted that once NPs reach the aerial parts, the risk of entering into the food chain increases (Dash and Kundu, 2020). Therefore, nanomaterials with agricultural purposes deserve particular attention (Khot et al., 2012), and a thorough knowledge of their mobility profiles is needed.

The behavior of NPs once inside plant tissues is poorly understood, and both positive and negative effects on plant growth have been documented (Rao and Shekhawat, 2016). There are reports on NPs phytotoxicity (Mazaheri-Tirani and Dayani, 2020) that describe oxidative stress in plants exposed to NPs (Marslin et al., 2017; Yanık and Vardar, 2018; Zhao et al., 2012), causing lipid peroxidation, as well as protein and DNA damage (reviewed by Arruda et al., 2015; Tripathi et al., 2017). However, several publications communicated some beneficial effects of NPs on crops (Aslani et al., 2014; Raliya and Tarafdar, 2013). For instance, peanut, rice, and perennial ryegrass biomass increased with low concentrations ($\leq$ 500 mg L^{-1}) of zerovalent iron NPs (Li et al., 2015; Guha et al., 2018; Huang et al., 2018). On the other hand, high concentrations ($>$ 1000 mg L^{-1}) of zerovalent iron NPs inhibited the growth of cattail, hybrid poplars, and rice (Ma et al., 2013; Wang et al., 2016).

This work aimed to determine if two important legume crops in Argentina, soybean and alfalfa, absorb and translocate citric acid-coated Fe_3O_4-NPs (from now on designated as Fe_3O_4-NPs) and if these nanoparticles display toxic effects on these species. Soybean is cultivated as a grain crop and represents the largest planted area for a legume in Argentina (Mur et al., 2018). Alfalfa is a central component of pastures dedicated to meat and dairy cattle in many regions.

2. Materials and methods

2.1. Nanoparticles synthesis

Fe_3O_4-NPs, 14 nm in size and hydrodynamic sizes in the range ~18 nm, were synthesized by coprecipitation, as described in De Sousa et al. (2013). Briefly, $FeCl_3{\cdot}6H_2O$ (10.2 mmol of Fe^{3+}) and $FeCl_2{\cdot}4H_2O$ (5.1 mmol of Fe^{2+}) were dissolved in 50 mL bi-distilled water, mixed, and heated to 60 °C. Then, 3 mL of NH_4OH solution (25% wt/vol) was added drop by drop and left to react for 30 min; at this point, the formation of Fe_3O_4 NPs was observed as a black precipitate. The mixture was left to grow while 75 mL of ammonia solution was added. Then, an aqueous solution of citric acid (0.02 g mL^{-1}) was added and left to react at 60 °C for 90 min. Finally, the citric acid-coated IO-NPs obtained were separated from the dispersion medium, washed several times, and resuspended in water at pH 7 to a final iron concentration of 18.1 mg mL^{-1}. The physical characterization, fully described in De Sousa et al. (2013), proved the formation of Fe_3O_4-NPs electrostatically stabilized by citric acid; citric acid molecules bind to the nanoparticle surfaces by one carboxylate group, leaving two others free and NPs negatively charged (Z-potential = − 36 mV). The morphology of these NPs under transmission electron microscopy (TEM) was already described, and the stability in water and Hoagland solution was previously corroborated (Iannone et al., 2016). Iron concentration in the colloidal sample was measured by titration.

2.2. Pre-sowing treatments and plant growth conditions

Soybean (*Glycine max* L.) seeds were provided by Nidera, Argentina, and alfalfa (*Medicago sativa* L.) seeds (Pampa Flor variety) were obtained from Guasch. Before sowing, the inert substrate selected (nutrient-free vermiculite) was irrigated with half-strength Hoagland (Hoagland and Arnon, 1950) solution (control, C) or half-strength Hoagland solution containing 50 or 100 mg L^{-1} of iron as Fe_3O_4-NPs (NP50 and NP100). These Fe_3O_4-NPs doses were selected considering data retrieved from previous reports (Rizwan et al., 2019; Tombuloglu et al., 2019a, 2019b). Two additional treatments in which soluble iron (as Fe-EDTA, also dissolved in half-strength Hoagland solution) was added to the inert substrate at final concentrations equal to those provided by Fe_3O_4-NPs were included (Fe50 and Fe100). Therefore, identical iron amounts under different chemical forms were applied only once at pre-sowing, making up four treatments: NP50, NP100, Fe50, Fe100. Six soybean and twenty alfalfa seeds were sown in each pot (1-L or 0.5-L capacity, respectively). The plant population obtained was uniform in all treatments. All the pots were distributed following a completely randomized design in a growth chamber (16/8 h photoperiod; 26/20 °C; fluorescent white light, photon flux density: 175 μmol m^2 s^{-1}) and watered every two days with half-strength standard Hoagland solution. Plants were harvested on day 26 after emergence. Roots, stems, and leaves were separately used for further analysis. Before magnetization measurements and biomass drying, roots were immersed in deionized water, sonicated for 5 s (Heat Systems, model W-375), and exhaustively washed with deionized water three times to remove the surface-adsorbed NPs, as described by Al-Amri et al. (2020).

2.3. Magnetization measurements

Dried plant tissues from control and treated plants were analyzed to determine specific magnetization (M) as a function of the applied magnetic field (H) at room temperature using a vibrating sample magnetometer (VSM, LakeShore 7404, maximum field of 18.000 Oe), as described by Wang et al. (2011). Magnetization measurements were performed in duplicate. For IO-NPs characterization, 40 μL of the colloidal suspension were sealed in a shrinkable sachet and measured at room temperature. The mean magnetic moment and saturation magnetization of the synthesized nanoparticles were obtained by fitting VSM data with a Langevin equation. The mean particle size was estimated from the mean magnetic moment, as described in De Sousa et al. (2013).

2.4. Iron determination

After drying at 80 °C up to constant weight, plant tissues were ground. The fine powder thus obtained was digested with a mixture of HNO_3:$HClO_4$ (3:1 vol/vol) at 170 °C, and Fe concentration in leaves and roots was determined by flame atomic absorbance spectrometry (Perkin Elmer AAnalyst 300, wavelength used: 248.3 nm, standard: AccuStandard 1000 ppm, linearity range: 6 mg L^{-1}, detection limit: 0.11 mg L^{-1}).

2.5. Seed germination and plant growth

The germination index of soybean and alfalfa seeds was recorded at 72 h by checking the coleoptiles emergence. On day 26 post-emergence, plant growth and several biochemical parameters, including oxidative stress biomarkers, were determined on fresh samples obtained from a pool of 25–30 plants per treatment.

Growth was evaluated by measuring shoots and roots length and fresh weight. The total root surface was estimated as previously described (Ansari et al., 1995). Briefly, roots were immersed in 0.05 M $NaNO_2$ for 10 s and then transferred to a beaker with a known amount of distilled water. An aliquot of this solution was subsequently collected to determine nitrite content by spectrophotometry at 540 nm after reaction with 1% of sulfanilamide in HCl and 0.02% of alpha-naphthyl ethylene diamine.

2.6. Chlorophyll content

Soybean and alfalfa leaf samples (100 mg FW) were incubated in 5 mL of 96% ethanol at 50–60 °C until complete discoloration. The absorbance at 654 nm in the ethanolic extracts was measured spectrophotometrically in a Hitachi U-2000 spectrophotometer, according to Wintermans and de Mots (1965). Chlorophyll (Chl) content was calculated using the following formula: Chl $a+b$ (μg mL^{-1}) = $A_{654}/39.8$.

2.7. Oxidative stress assessment

2.7.1. In situ determination of reactive oxygen species: $O_2^{\cdot-}$ and H_2O_2 localization

Accumulation of superoxide anion ($O_2^{\cdot-}$) was estimated using a 0.05% (wt/vol) solution of nitroblue tetrazolium (NBT), which reacts with $O_2^{\cdot-}$ and produces a blue precipitate of formazan. Diphenylene iodonium (DPI, an NADPH oxidase inhibitor that prevents $O_2^{\cdot-}$ production) was used as a negative control (Bolwell et al., 1998; Frahry and Schopfer, 1998). H_2O_2 accumulation was also determined in situ by a histochemical method using 3,3′ diaminobenzidine (DAB) as the revealing agent. The presence of brown spots was indicative of H_2O_2 accumulation (Thordal-Christensen et al., 1997). Ascorbic acid (a well-known antioxidant) was used as a negative control.

2.7.2. Thiobarbituric acid reactive substances (TBARS) determination

Lipid peroxidation was determined by estimating thiobarbituric acid reactive substances (TBARS), as described by Heath and Packer (1968). Fresh leaves or roots (0.3 g) were homogenized in 3 mL of 20% (wt/vol) trichloroacetic acid (TCA). The homogenate was centrifuged at 15,000 rpm for 20 min, and 1 mL-supernatant aliquots were mixed with 1 mL of 20% (wt/vol) TCA containing 0.5% (wt/vol) of thiobarbituric acid and 100 μL of 4% (wt/vol) butyl hydroxytoluene in ethanol. The mixture was heated at 95 °C for 25 min and cooled on ice. After centrifuging at 4,000 rpm for 3 min, TBARS were measured spectrophotometrically at 532 nm by subtracting the turbidity at 600 nm. TBARS content was calculated using the extinction coefficient of malondialdehyde (155 mM^{-1} cm^{-1}).

2.7.3. Enzyme assays

Plant homogenates were prepared in 50 mM phosphate buffer pH 7.8 containing 0.5 mM EDTA, 1 g PVP, and 0.5% (vol/vol) Triton X-100. Catalase (CAT, EC 1.11.1.6) activity was determined as described by Chance et al. (1979), and guaiacol peroxidase (GPOX, EC 1.11.1.7) activity was determined according to Maehly and Chance (1954). Ascorbate peroxidase (APOX, EC 1.11.1.11) activity was determined immediately after extraction, according to Nakano and Asada (1981).

2.8. Cell viability and membrane damage assessments

2.8.1. Evans blue staining

The proportion of cells undergoing cell death process was estimated through this staining, as previously described (Baker and Mock, 1994). Briefly, roots and leaves were incubated with 0.25% (wt/vol) of an aqueous solution of Evans Blue for 15 min at room temperature, then washed twice with distilled water and left in distilled water overnight. The following day, the samples were incubated for 1 h at 50 °C with a methanol-SDS solution, and the absorbance at 595 nm was measured.

2.8.2. Electrolyte leakage

Oxidative damage to membranes can result in increased electrolyte leakage. Root and shoot samples were kept in vials with deionized water for 1 h, and the electrical conductivity (EC) (T1) was measured. Subsequently, the material was heated at 100 ºC for 1 h, and the EC was determined again (T2). The relative electrical conductivity was calculated as (T1/T2) x 100, as described by Shou et al. (2004).

2.9. Statistics

All data presented are mean values of three independent sets of experiments; standard errors (SE) are included. Statistical analysis was carried out by one-way ANOVA followed by Tukey's multiple range test. Asterisks indicate significant differences (* $p < 0.05$, two asterisks ** $p < 0.01$, and three asterisks *** $p < 0.001$).

3. Results

3.1. Fe_3O_4-NPs distribution in plant tissues

To evaluate the uptake and translocation of Fe_3O_4-NPs, the magnetization vs. the applied magnetic field (M-H) was measured using a vibrating sample magnetometer. The M-H measurements were divided by the mass of the sample; therefore, the magnetic signal would couple to the content of IO-NPs. Ferromagnetic nanomaterials with a size minor to 10–20 nm are superparamagnetic; this phenomenon usually occurs only in NPs systems (Huber, 2005).

First, the superparamagnetic behavior of our citric acid-coated Fe_3O_4-NPs was corroborated through VSM measurements. The VSM data shows a sigmoid-shaped curve fitting with a Langevin function, indicating the superparamagnetic behavior (Fig. 1A). From the fit, a saturation magnetization (Ms) of 16.8 ± 0.3 emu g_{Fe}^{-1} and a particle mean magnetic moment ($\langle\mu\rangle$) of 26,350 μ_B were inferred. Using the formula $V = \frac{\langle\mu\rangle}{Ms}$, where $V = \frac{\pi d^3}{6}$ is the nanoparticle volume and d is its diameter, a mean size of 14 ± 4 nm was obtained.

Fig. 1B shows VSM measurements in soybean roots. It may be noticed that C, Fe50, and Fe100 samples presented a diamagnetic behavior (straight line), characteristic of organic materials, while NP50 and NP100 samples exhibited a superparamagnetic behavior (sigmoidal curve) overlapping the diamagnetic one. Fig. 1C and D show the VSM measurements performed in stem and leaf samples of soybean plants, respectively. A diamagnetic signal was mainly observed in these samples, irrespective of the pre-sowing treatment, revealing negligible translocation of Fe_3O_4-NPs to the aerial parts. A more intense superparamagnetic signal was detected in alfalfa roots exposed to Fe_3O_4-NPs (Fig. 1E). These results indicated that Fe_3O_4-NPs were uptaken by both legumes. Diamagnetic signals were found under the other pre-sowing treatments. In alfalfa stems and leaves, a weak superparamagnetic signal was found (Fig. 1 F,G).

3.2. Total iron content

Total Fe content in the leaves of soybean increased significantly only when soluble iron was added at pre-sowing (about a 2–3-fold increase), whereas in the leaves of alfalfa, total iron content increased upon the addition of both iron-containing compounds, being the increase more pronounced with the soluble form (Table 1). Total iron concentration in the roots increased significantly under all treatments in both legumes

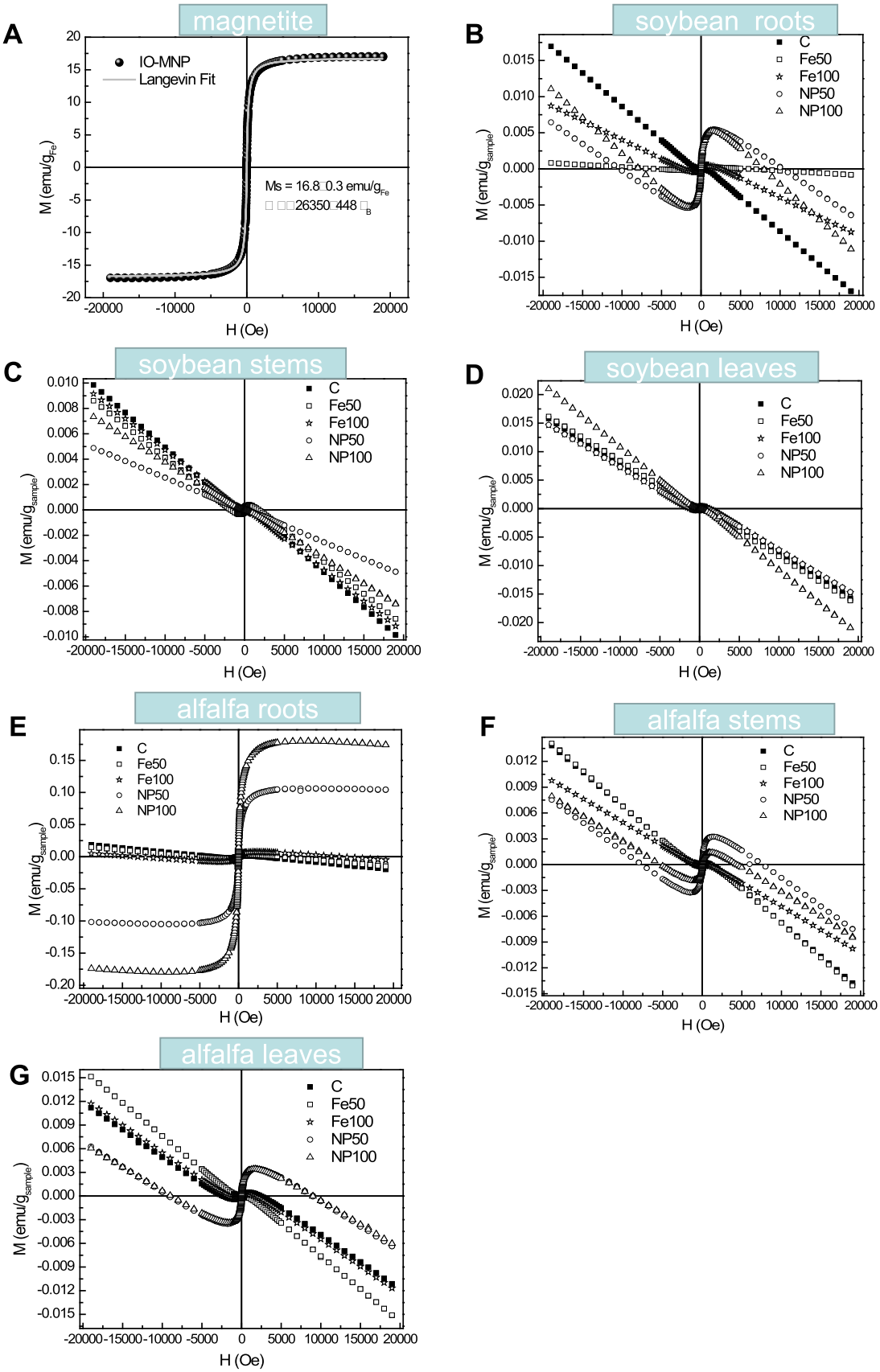

Fig. 1. Selected magnetization results of vibrating sample magnetometry (VSM) analyses. Magnetization loops are shown as specific magnetization M vs. applied field H. Fe_3O_4-NPs suspension (A); root samples of soybean (B) and alfalfa (E); stem samples of soybean (C) and alfalfa (F); leaf samples of soybean (D) and alfalfa (G). M (emu g^{-1} DW) and H (Oe) represent the magnetization and the applied magnetic field, respectively. C: control plants; NP50, NP100, Fe50, and Fe100: plants grown on an inert substrate that received once, at pre-sowing, 50 or 100 mg Fe L^{-1} supplied as Fe_3O_4-NPs or Fe-EDTA, dissolved in half-strength Hoagland solution.

Table 1
Total iron content.

Iron content (mg g^{-1} DW)						
	Plant tissue	C	Fe50	Fe100	NP50	NP100
Soybean	Root	0.35 ± 0.02	1.61 ± 0.03***	1.75 ± 0.03***	1.35 ± 0.04***	1.65 ± 0.02***
	Leaf	0.06 ± 0.02	0.11 ± 0.02**	0.16 ± 0.03**	0.05 ± 0.02	0.07 ± 0.02
Alfalfa	Root	0.43 ± 0.03	1.22 ± 0.02**	1.41 ± 0.03**	0.94 ± 0.03**	1.32 ± 0.04***
	Leaf	0.13 ± 0.02	0.28 ± 0.05**	0.35 ± 0.03**	0.20 ± 0.04*	0.22 ± 0.06 *

C: control plants; NP50, NP100, Fe50, and Fe100: plants grown on an inert substrate which received once, at pre-sowing, 50 or 100 mg Fe L^{-1} supplied as Fe_3O_4-NPs or Fe-EDTA, dissolved in half-strength Hoagland solution.
Data are the mean ± SE of three independent experiments, with five replicates per treatment. Asterisks within rows indicate significant differences (*$p < 0.05$; **$p < 0.01$; ***$p < 0.001$), according to Tukey's multiple-range test.

examined (about a 2–5-fold increase compared to control plants).

3.3. Germination, plant growth, and chlorophyll content

The germination index of soybean and alfalfa was not significantly affected by any pre-sowing treatment tested (Fig. 2). Iron addition in both chemical forms (as Fe_3O_4-NPs or Fe-EDTA) increased the shoot biomass accumulation in these legumes by about 40% ($p < 0.01$) and 20% ($p < 0.05$), respectively, with no differences between doses (Table 2). Root fresh weight also increased due to the application of these Fe-containing compounds at pre-sowing, being the increase rate more pronounced for Fe_3O_4-NPs than Fe-EDTA, but not affected by the dose. Alfalfa root length also increased around 50% in plants exposed to these Fe-containing compounds, irrespective of the chemical form and dose ($p < 0.01$); however, soybean root length increased when Fe_3O_4-NPs were applied only. Root surface increased very significantly both in soybean (~50% at both NPs doses, $p < 0.001$) and alfalfa (63% and 97% at NP50 and NP100, respectively, $p < 0.001$) (Table 2). Also, Fe application as Fe_3O_4-NPs or Fe-EDTA at pre-sowing increased chlorophyll content in both legume species. The maximum increase over the control was observed under NP50 for alfalfa (26%) and under NP50 or NP100 for soybean (both 40%), $p < 0.001$ (Fig. 3).

3.4. Oxidative stress and antioxidant parameters

Neither Fe_3O_4-NPs nor Fe-EDTA addition produced significant changes in superoxide anion ($O_2^{\cdot-}$) and hydrogen peroxide accumulation in roots or leaves (data not shown). Accordingly, no increases in TBARS levels (indicative of lipid peroxidation) were observed in the roots or shoots of Fe_3O_4-NPs-exposed soybean plants (Fig. 4A). Moreover, Fe addition in both forms tended to reduce TBARS levels in alfalfa plants, mainly in the aerial part (Fig. 4D). Cell viability and permeability did not change due to the pre-sowing treatments in the plant species evaluated (Fig. 4B, C, E, F).

The only change in the enzymatic antioxidant machinery was found for CAT, whose activity increased consistently under Fe_3O_4-NPs treatments in roots (~30–50%, $p < 0.05/0.01$) and shoots (~30%, $p < 0.05$) of both plant species. APOX and GPOX activities showed no significant changes (Table 3).

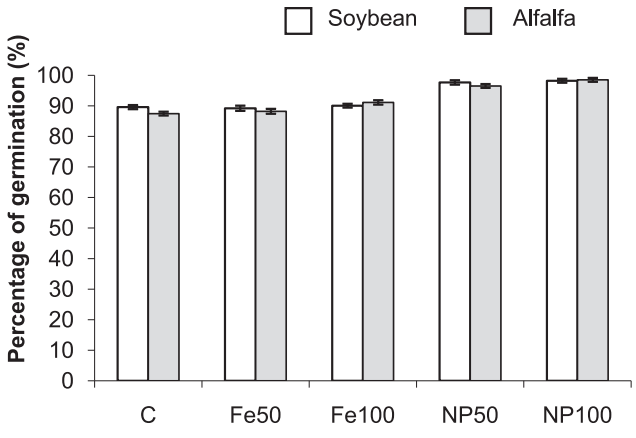

Fig. 2. Germination index of soybean and alfalfa. C: control plants; NP50, NP100, Fe50, and Fe100: plants grown on an inert substrate that received once, at pre-sowing, 50 or 100 mg Fe L^{-1} supplied as Fe_3O_4-NPs or Fe-EDTA, dissolved in half-strength Hoagland solution. Mean values and standard errors of three independent experiments (n = 10) are shown. Asterisks indicate significant differences (*, $p < 0.05$; **, $p < 0.01$; ***, $p < 0.001$), according to Tukey's multiple range test.

4. Discussion

The increasing use of nanoparticles demands better comprehension of the physicochemical and biological phenomena regulating their dynamics in the environment and inside plant tissues. In this work, the effect of adding magnetite nanoparticles coated with citric acid in the inert substrate where soybean and alfalfa were subsequently grown was evaluated at 26 days after emergence.

Since IO-NPs have magnetic properties, their presence in different plant tissues was analyzed by VSM analysis (Fig. 1). Our magnetization studies, along with the iron content analysis, suggest that Fe_3O_4-NPs were absorbed by the roots of the species examined, but they were not translocated (soybean) or only translocated in minimal amounts (alfalfa) from roots to shoots.

This result has an important practical consequence: at the dose applied, which may represent a mild accumulation condition, these nanoparticles are not expected to enter into the chain food, as they do not migrate significantly to the shoots. In this way, the risk of toxicity to humans or animals becomes negligible. The uptake of IO-NPs with no translocation to the leaves has been shown before in other plant species such as ryegrass, pumpkin (Wang et al., 2011), cucumber (Konate et al., 2018), *Citrus maxima* (Li et al., 2018), and summer squash (Tombuloglu et al., 2019b). In our previous work, these same nanoparticles did not translocate to the aerial part in wheat plants (Iannone et al., 2016).

Though our citric acid-coated IO-NPs were stable as a colloidal solution at pH 7, at a lower pH such as that of the root apoplast and in the presence of many other solutes, aggregation phenomena may exist and limit NPs passage through plasmodesmata as well as NPs translocation through the vascular system (Iannone et al., 2016). In this sense, it is interesting to note that Sun et al. (2019) reported the formation of aggregates mainly composed of iron deposited in the adjacent regions of cell walls and cell membranes of mung bean roots exposed to high concentrations of bare and starch-stabilized zerovalent iron nanoparticles, and suggested that both aggregation and internalization of nanoparticles in root cells may occur, resulting in relatively less translocation and phytotoxicity. Nanoparticles translocation inside plants is expected to depend on their concentration, size, and type, and particularly, on their net electrical charge. However, the plant species is probably an important issue, which was not addressed in depth. Quantitative and qualitative differences among plant species in plant root exudates and sap composition might be relevant in terms of Fe_3O_4-NPs

Table 2
Growth parameters.

Plant specie	Treatment	Root surface (nmol nitrite plant^{-1})	Root length (cm)	Shoot length (cm)	Root weight (g)	Shoot weight (g)
Soybean	C	43,093.18 ± 3104.39	18.50 ± 0.91	22.08 ± 0.51	0.94 ± 0.16	2.39 ± 0.43
	Fe50	49,096.28 ± 4267.03	21.12 ± 0.82	22.50 ± 0.68	1.35 ± 0,17**	3.30 ± 0.37**
	Fe100	50,114.25 ± 3432.18	21.71 ± 1.03	22.60 ± 0.64	1.40 ± 0.15**	3.27 ± 0.30**
	NP50	64,923.55 ± 4813.42***	23.14 ± 1.00*	23.25 ± 0.55	1.64 ± 0.16***	3.36 ± 0.29**
	NP100	65,577.65 ± 3232.23***	23.52 ± 0.82*	23.41 ± 0.58	1.72 ± 0.17***	3.41 ± 0.37**
Alfalfa	C	348.06 ± 49.22	5.05 ± 0.66	10.44 ± 0.51	0.013 ± 0.002	0.114 ± 0.006
	Fe50	269.08 ± 36.14	7.11 ± 0.67**	11.26 ± 0.66	0.019 ± 0.004*	0.130 ± 0.011*
	Fe100	377.51 ± 34.70	7.47 ± 0.77**	11.52 ± 0.33	0.018 ± 0.004*	0.142 ± 0.013*
	NP50	567.60 ± 33.17***	7.72 ± 0.80**	11.37 ± 0.36	0.028 ± 0.005**	0.131 ± 0.008*
	NP100	686.75 ± 48.59***	8.05 ± 0.58**	11.63 ± 0.41	0.026 ± 0.002**	0.137 ± 0.010*

C: control plants, NP50, NP100, Fe50, Fe100: plants grown on an inert substrate which received once, at pre-sowing, 50 or 100 mg Fe L^{-1} supplied as Fe_3O_4-NPs or Fe-EDTA, dissolved in half-strength Hoagland solution.
Values are the mean ± SE of three independent experiments, with ten replicates per treatment. Asterisks within rows indicate significant differences (*$p < 0.05$, **$p < 0.01$, ***$p < 0.001$), according to Tukey's multiple-range test.

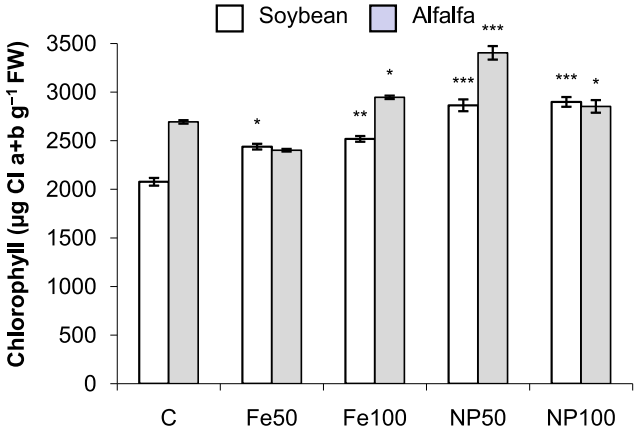

Fig. 3. Chlorophyll content in soybean and alfalfa leaves. C: control plants; NP50, NP100, Fe50, and Fe100: plants grown on an inert substrate that received once, at pre-sowing, 50 or 100 mg Fe L^{-1} supplied a Fe_3O_4-NPs or Fe-EDTA, dissolved in half-strength Hoagland solution. Mean values and standard errors of three independent experiments (n = 10) are shown. Asterisks indicate significant differences (* $p < 0.05$; ** $p < 0.01$; *** $p < 0.001$), according to Tukey's multiple range test.

plant entry and translocation. Further studies to shed light on the actual occurrence of Fe_3O_4-NPs aggregation/precipitation phenomena in the legumes evaluated are necessary.

In contrast to our findings, Ghafariyan et al. (2013) found superparamagnetic signals in stems and leaves of soybean plants exposed to higher concentrations of iron oxide NPs, with various surface charges. Zhu et al. (2012) observed that Au NPs could accumulate in *Oryza sativa* shoots, unlike *Raphanus raphanistrum* and *Cucurbita pepo* shoots. These authors also reported that the positively charged Au NPs were more easily uptaken by plant roots than the negatively charged ones. On the other hand, it is supposed that ion transporters in the cell membrane can partially be involved in the uptake of metallic-based NPs (Rico et al., 2011). However, there is still no conclusive research about NPs uptake by plants and transport inside plant tissues (Servin et al., 2015). According to a recent report, plant species, NPs characteristics (shape, size, charge), and the growth media influence the capability of IO-NPs to be translocated into plant organs (Al-Amri et al., 2020).

An interesting finding is that in both legumes tested, root surface increased very significantly when plants developed in vermiculite amended with Fe_3O_4-NPs, but not with Fe-EDTA. This suggests an effect of the nanostructure itself on root hair formation. Root hairs are key determinants of the effective absorption area for terrestrial plants. Differentiation of root epidermal cells into root hairs is a complex process in which plant hormone balance plays a crucial role. In recent years, the effects of these new materials on plant hormone levels have started being investigated. Le Van et al. (2015) observed that CeO_2 NPs had no significant effect on indole-3-acetic acid (IAA) and other hormones in cotton leaves, whereas Gui et al. (2015) reported increased IAA levels in rice roots in response to maghemite (γFe_2O_3) application. Rui et al. (2016) also informed increments in several phytohormones such as gibberellins (including GA7 and GA3) and trans-zeatin riboside upon Fe_2O_3 NPs addition in peanut plants, while Hao et al. (2016) communicated decreases in phytohormone contents in rice seedlings related to the application of carbon nanotubes. ZnO nanoparticles were also reported to decrease cytokinins and auxins in *Arabidopsis thaliana* apices, leading to strong growth inhibition (Vanková et al., 2017). To our knowledge, this is the first report showing a positive effect of citric acid-coated IO-NPs on total root surface area.

Considering that both iron-containing compounds led to increased plant biomass, iron seems to be a key factor in the growth-stimulating effect observed. In this sense, several iron-dependent steps in chlorophyll biosynthesis have been reported (Miller et al., 1995). Yuan et al. (2018) found that low doses of Fe NPs promoted *Capsicum annuum* growth by modifying leaf organization and increasing the chloroplast number and grana stacking, apart from regulating vascular bundles development. On the other hand, NPs are known to augment the water uptake capacity by altering the membrane pores or ion channels (Zhu et al., 2008), a phenomenon that would explain the higher fresh weight observed in soybean and alfalfa roots exposed to Fe_3O_4-NPs, in coincidence with those previously reported (Zhu et al., 2008; Al-Amri et al., 2020). Root biomass and water content also increased in radish exposed to citric acid-coated CeO_2 NPs (Trujillo-Reyes et al., 2013).

In previous works (Kim et al., 2014, 2015), zerovalent iron NPs induced cell-wall loosening in Arabidopsis roots and leaves, leading to increased shoot and root elongation. According to those authors, iron NPs triggered high plasma membrane H^+-ATPase (PM H^+-ATPase) activity, which resulted in increased leaf area and enhanced stomatal opening, which facilitates CO_2 uptake and favors photosynthesis. It was proposed that the iron NPs-induced activation of PM H^+-ATPase in roots promotes auxin transport, and this may result in PM H^+-ATPase activation in shoots (Kim et al., 2015).

In the present work, Fe_3O_4-NPs increased CAT activity in the roots and shoots of both legumes analyzed. In *Gossypium hirsutum*, ZnO NPs treatments increased SOD and POX activities, with a subsequent decrease in lipid peroxidation (Venkatachalam et al., 2017). We previously found that the activity of several antioxidant enzymes (CAT, GPOX, APOX, and SOD) was increased in the roots and shoots of wheat plants exposed to the same nanoparticles, even when these nanoparticles were not translocated to the aerial part (Iannone et al., 2016). Similarly, SOD and CAT activity increased in the roots and shoots of ryegrass and pumpkin plants exposed to magnetite NPs, despite the lack of nanoparticles translocation to leaves (Wang et al., 2011).

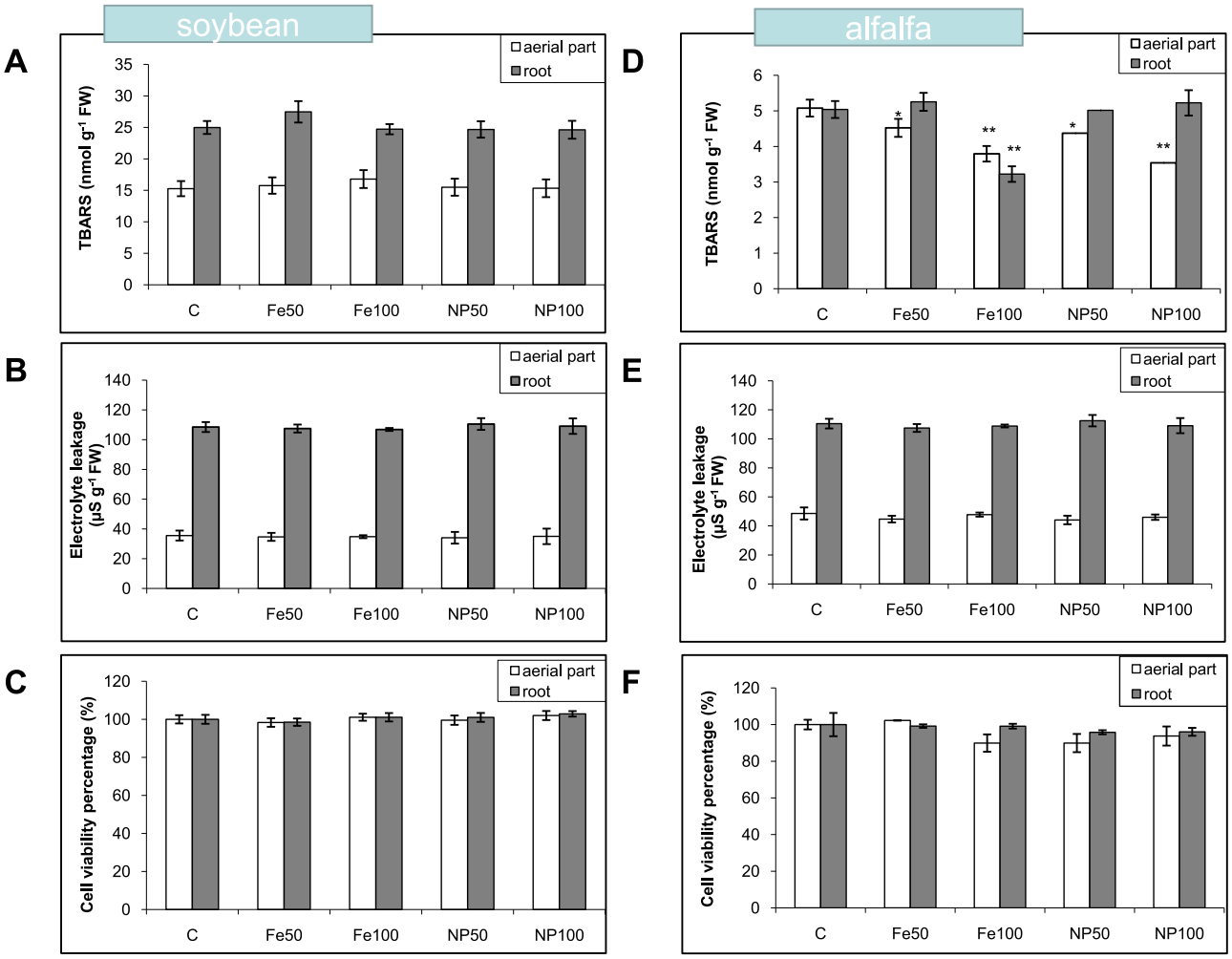

Fig. 4. TBARS content (A, D), electrolyte leakage (B, E), and cell viability percentage (C, F) in shoots (white) and roots (gray) of soybean and alfalfa seedlings. C: control plants; NP50, NP100, Fe50, and Fe100: plants grown on an inert substrate that received once, at pre-sowing, 50 or 100 mg Fe L^{-1} supplied as Fe_3O_4-NPs or Fe-EDTA, dissolved in half-strength Hoagland solution. Mean values and standard errors of three independent experiments (n = 6) are shown. Asterisks indicate significant differences (* $p < 0.05$; ** $p < 0.01$), according to Tukey's multiple range test.

Table 3
Antioxidant enzymes activities in plant tissues.

		Soybean		Alfalfa	
		Aerial part	Root	Aerial part	Root
CAT (pmol g^{-1} FW s^{-1})	C	0.51 ± 0.02	0.33 ± 0.05	0.70 ± 0.03	0.58 ± 0.06
	Fe50	0.45 ± 0.09	0.40 ± 0.07*	0.77 ± 0.06	0.60 ± 0.10
	Fe100	0.54 ± 0.03	0.38 ± 0.08	0.65 ± 0.05	0.50 ± 0.09
	NP50	0.67 ± 0.06*	0.45 ± 0.04*	0.87 ± 0.02*	0.73 ± 0.04*
	NP100	0.70 ± 0.04*	0.50 ± 0.05**	0.96 ± 0.09*	0.76 ± 0.07*
APOX (nmol g^{-1} FW s^{-1})	C	1.75 ± 0.22	6.51 ± 0.28	3.31 ± 0.40	8.31 ± 0.36
	Fe50	1.81 ± 0.33	6.44 ± 0.30	3.25 ± 0.26	8.40 ± 0.40
	Fe100	1.95 ± 0.15	6.68 ± 0.24	3.39 ± 0.35	8.49 ± 0.30
	NP50	1.83 ± 0.12	6.82 ± 0.12	3.41 ± 0.34	8.70 ± 0.19
	NP100	1.97 ± 0.25	6.98 ± 0.20	3.50 ± 0.31	8.83 ± 0.39
GPOX (nmol g^{-1} FW)	C	20.81 ± 0.11	6.27 ± 0.03	24.42 ± 0.11	4.81 ± 0.29
	Fe50	20.85 ± 0.09	6.40 ± 0.16	25.01 ± 0.33	4.90 ± 0.12
	Fe100	20.89 ± 0.08	6.18 ± 0.09	24.60 ± 0.30	4.95 ± 0.15
	NP50	20.73 ± 0.15	6.12 ± 0.23	24.35 ± 0.22	4.70 ± 0.20
	NP100	20.67 ± 0.20	6.17 ± 0.14	24.29 ± 0.21	4.58 ± 0.31

C: control plants; NP50, NP100, Fe50, and Fe100: plants grown on an inert substrate which received once, at pre-sowing, 50 or 100 mg Fe L^{-1} supplied as Fe_3O_4-NPs or Fe-EDTA, dissolved in half-strength Hoagland solution.
Data are the mean ± S.E. of two independent experiments, with five replicates per treatment. Asterisks indicate significant differences (* $p < 0.05$; ** $p < 0.01$) according to Tukey's multiple range test. Enzymatic activities were assayed as described in Materials and Methods. One unit of CAT is the amount of the enzyme that oxidizes 1 pmol of H_2O_2 min^{-1} under the assay conditions. One unit of APOX forms 1 nmol of oxidizes ascorbate min^{-1} under the assay conditions. One unit of GPOX is the amount of the enzyme that reduces 1 nmol of H_2O_2 min^{-1} under the assay conditions.

Ngan et al. (2020) reported that the increased root elongation and better absorption efficiency in carnation plants exposed to iron NPs could be attributed to cell-wall loosening induced by $OH^{-\cdot}$ radicals. These authors also described that iron NPs increased SOD, CAT, and APX activities and enhanced carnation plants' growth. Additionally, Fe_2O_3 NPs promoted peanut growth by regulating phytohormone contents and antioxidant enzyme activities, resulting in adequate ROS amounts capable of acting as signaling molecules for root elongation and plant development (Rui et al., 2016).

We highlight that neither oxidative damage nor cell death symptoms were observed in soybean or alfalfa plants treated with these citric acid-coated Fe_3O_4-NPs at final Fe concentrations of 50 and 100 mg L^{-1}. These results are in accordance with those reported by Ghafariyan et al. (2013), who tested IO-NPs at higher concentrations. Moreover, under our experimental system, instead of being toxic, Fe_3O_4-NPs improved plant growth and increased chlorophyll contents. Similar positive effects were also found in maize plants exposed to hematite and ferrihydrite (Pariona et al., 2017) and in wheat plants exposed to IO-NPs (Yasmeen et al., 2015).

In the same way, Yan et al. (2020) found that Fe_3O_4 NPs increased root length and reduced TBARS levels in maize plants. Besides, it was observed that Fe_2O_3 NPs considerably boosted the growth in tomato (Shankramma et al., 2016), watermelon (Li et al., 2013), corn (Li et al., 2016), sorghum (Maswada et al., 2018), and rapeseed (Palmqvist et al., 2017). In line with these findings, wheat seeds primed with ZnO NPs or IO-NPs at similar concentrations to those used in this work showed a positive effect on several photosynthesis parameters (chlorophyll *a* and *b* contents, stomatal conductance, photosynthetic rate) and mitigated the adverse effect of Cd stress (Rizwan et al., 2019). Also, Golshahi et al. (2018) observed that polymeric monodisperse IO-NPs led to chlorophyll increments, with improvements in the plasmatic membrane stability index of root and shoot cells, along with increased levels of micronutrients (Fe, Zn, and Cu). Fe_2O_3 NPs also improved peppermint performance under saline stress (Askary et al., 2017). Li et al. (2013) reported that IO-NPs improved the physiological function and resistance to environmental stresses in watermelon, whereas H_2O_2 content and lipid peroxidation were reduced in *Brassica napus* plants subjected to γ-Fe_2O_3 nanoparticles and exposed to drought (Palmqvist et al., 2017). However, other NPs such as ZnO and CuO used at higher concentrations (500 mg L^{-1}) had adverse effects on soybean development (López-Moreno et al., 2010; Nair and Chung, 2014). Specifically, CuO NPs led to an increased ROS production, which activated the soybean antioxidant system (Nair and Chung, 2014). These results corroborate the importance of the doses applied when assessing plants' responses to these new materials.

5. Conclusion

In the present work, we demonstrated that soybean and alfalfa plants absorbed citric acid-coated magnetite nanoparticles and accumulated them in their roots, with little or no translocation to the aerial parts. This low mobility inside plants becomes a positive trait, considering that aerial organs (leaves and grains) are commonly consumed as food by humans and animals. On the other hand, we showed that when applied at iron concentrations up to 100 mg L^{-1}, citric acid-coated magnetite nanoparticles showed positive effects on plant growth, particularly on root hair formation and chlorophyll concentration, two key plant features with a direct impact on net plant productivity.

CRediT authorship contribution statement

María Florencia Iannone: Conceptualization, Methodology, Formal analysis, Investigation, Writing - original draft, Writing - review & editing, Funding acquisition. **María Daniela Groppa**: Writing - original draft, Review. **Myriam Sara Zawoznik**: Conceptualization, Writing - original draft, Writing - review & editing. **Diego Fernando Coral**: Investigation, Formal analysis, Review. **Marcela Beatriz Fernández van Raap**: Formal analysis, Review. **María Patricia Benavides**: Resources, Funding acquisition, Review.

Declaration of Competing Interest

The authors declare that they have no known competing financial interests or personal relationships that could have appeared to influence the work reported in this paper.

Acknowledgments

This work was supported by the University of Buenos Aires (Project UBACYT 20020150200008BA) and CONICET (PIP GI 11220120100266). Nanoparticle synthesis and magnetic analysis were performed at the Instituto de Física La Plata (IFLP)/Universidad Nacional de La Plata (UNLP), Argentina. Iannone MF, Groppa MD, Benavides MP and Fernández van Raap MB are researchers of Consejo Nacional de Investigaciones Científicas y Técnicas (CONICET). Zawoznik MS is a researcher at the Universidad de Buenos Aires (UBA).

References

Al-Amri, N., Tombuloglu, H., Slimani, Y., Akhtar, S., Barghouthi, M., Almessiere, M., Alshammari, T., Baykal, A., Sabit, H., Ercan, I., Ozcelik, S., 2020. Size effect of iron (III) oxide nanomaterials on the growth, and their uptake and translocation in common wheat (*Triticum aestivum* L.). Ecotoxicol. Environ. Saf. 194, 110377.

Ali, A., Zafar, H., Zia, M., Ul Haq, I., Phull, A.R., Ali, J.S., Hussain, A., 2016. Synthesis, characterization, applications, and challenges of iron oxide nanoparticles. Nanotechnol. Sci. Appl. 9, 49–67.

Ansari, S.A., Kumar, P., Gupta, B.N., 1995. Root surface area measurements based on adsorption and desorption of nitrite. Plant Soil 175, 133–137.

Arruda, S.C.C., Silva, A.L.D., Galazzi, R.M., Azevedo, R.A., Arruda, M.A.Z., 2015. Nanoparticles applied to plant science: a review. Talanta 131, 693–705.

Askary, M., Talebi, S.M., Amini, F., Dousti, A., Bangan, B., 2017. Effects of iron nanoparticles on *Mentha piperita* L. under salinity stress. Biologija 63, 65–75.

Aslani, F., Bagheri, S., Muhd Julkapli, N., Juraimi, A.S., Hashemi, F.S.G., Baghdadi, A., 2014. Effects of engineered nanomaterials on plants growth: an overview. Sci. World J. 2014, 1–28.

Attia, T.M.S., Elsheery, N.I., 2020. Nanomaterials: scope, applications, and challenges in agriculture and soil reclamation. In: Hayat, S., Pichtel, J., Faizan, M., Fariduddin, Q. (Eds.), Sustainable Agriculture Reviews, 41. Springer, Cham.

Baker, C.J., Mock, N.M., 1994. An improved method for monitoring cell death in cell suspension and leaf disc assays using Evans blue. Plant Cell Tissue Organ Cult. 39, 7–12.

Bolwell, G.P., Davies, D.R., Gerrish, C., Auh, C.-K., Murphy, T.M., 1998. Comparative biochemistry of the oxidative burst produced by rose and French bean cells reveals two distinct mechanisms. Plant Physiol. 116, 1379–1385.

Chance, B., Sies, H., Boveris, A., 1979. Hydroperoxide metabolism in mammalian organs. Physiol. Rev. 59, 527–605.

Chen, H., 2018. Metal based nanoparticles in agricultural system: behavior, transport, and interaction with plants. Chem. Speciat. Bioavailab. 30, 123–134.

Dash, S.R., Kundu, C.N., 2020. Promising opportunities and potential risk of nanoparticle on the society. IET Nanobiotechnol. 14, 253–260.

De Sousa, M.E., Fernandez van Raap, M.B., Rivas, P.C., Mendoza Zélis, P., Girardin, P., Pasquevich, G.A., Alessandrini, J.L., Muraca, D., Sánchez, F.H., 2013. Stability and relaxation mechanisms of citric acid coated magnetite nanoparticles for magnetic hyperthermia. J. Phys. Chem. C 117, 5436–5445.

Frahry, G., Schopfer, P., 1998. Inhibition of $O_2^{\cdot-}$- reducing activity of horseradish peroxidase by diphenyleneiodonium. Phytochemistry 48, 223–227.

Ghafariyan, M.H., Malakouti, M.J., Dadpour, M.R., Stroeve, P., Mahmoudi, M., 2013. Effects of magnetite nanoparticles on soybean chlorophyll. Environ. Sci. Technol. 47, 10645–10652.

Gladkova, M.M., Terekhova, V.A., 2013. Engineered nanomaterials in soil: sources of entry and migration pathways. Mosc. Univ. Soil Sci. Bull. 68, 129–134.

Golshahi, S., Ahangar, A.G., Mir, N., Ghorbani, M., 2018. A comparison of the use of different sources of nanoscale iron particles on the concentration of micronutrients and plasma membrane stability in sorghum. Soil Sci. Plant Nutr. 18, 236–252.

Govea-Alcaide, E., Masunaga, S.H., De Souza, A., Fajardo-Rosabal, L., Effenberger, F.B., Rossi, L.M., Jardim, R.F., 2016. Tracking iron oxide nanoparticles in plant organs using magnetic measurements. J. Nanopart. Res. 18, 305.

Guha, T., Ravikumar, K., Mukherjee, A., Mukherjee, A., Kundu, R., 2018. Nanopriming with zero valent iron (nZVI) enhances germination and growth in aromatic rice cultivar (*Oryza sativa* cv. Gobindabhog L.). Plant Physiol. Biochem. 127, 403–413.

Gui, X., Deng, Y., Rui, Y., Gao, B., Luo, W., Chen, S., Van Nhan, L., Li, X., Liu, S., Han, Y., Liu, L., Xing, B., 2015. Response difference of transgenic and conventional rice (Oryza sativa) to nanoparticles (γFe2O3). Environ. Sci. Pollut. Res. 22, 17716–17723.

Hao, Y., Yu, F., Lv, R., Ma, C., Zhang, Z., Rui, Y., Liu, L., Cao, W., Xing, B., Choi, J., 2016. Carbon nanotubes filled with different ferromagnetic alloys affect the growth and development of rice seedlings by changing the C:N ratio and plant hormones concentrations. PLoS One 11, e0157264.
Heath, R.L., Packer, L., 1968. Photoperoxidation in isolated chloroplasts. I. Kinetics and stoichiometry of fatty acid peroxidation. Arch. Biochem. Biophys. 125, 189–198.
Hoagland, D.R., Arnon, D.I., 1950. The water–culture method for growing plants without soil. Circular, University of California, College of Agriculture, Agricultural Experiment Station 347, 42.
Huang, D., Qin, X., Peng, Z., Liu, Y., Gong, X., Zeng, G., Huang, C., Cheng, M., Xue, W., Wang, X., 2018. Nanoscale zerovalent iron assisted phytoremediation of Pb in sediment: impacts on metal accumulation and antioxidative system of Lolium perenne. Ecotoxicol. Environ. Saf. 153, 229–237.
Huber, D.L., 2005. Synthesis, properties, and applications of iron nanoparticles. Small 1 (5), 482–501.
Iannone, M.F., Groppa, M.D., De Sousa, M.D., Fernández van Raap, M.B., Benavides, M. P., 2016. Impact of magnetite iron oxide nanoparticles on wheat (Triticum aestivum L.) development: evaluation of oxidative damage. Environ. Exp. Bot. 131, 77–88.
Khot, L.R., Sankaran, S., Maja, J.M., Ehsani, R., Schuster, E.W., 2012. Applications of nanomaterials in agricultural production and crop protection: a review. Crop Prot. 35, 64–70.
Kim, J.H., Lee, Y., Kim, E.J., Gu, S., Sohn, E.J., Seo, Y.S., An, H.J., Chang, Y.-S., 2014. Exposure of iron nanoparticles to Arabidopsis thaliana enhances root elongation by triggering cell wall loosening. Environ. Sci. Technol. 48 (6), 3477–3485.
Kim, J.H., Oh, Y., Yoon, H., Hwang, I., Chang, Y.S., 2015. Iron nanoparticle induced activation of plasma membrane H+-ATPase promotes stomatal opening in Arabidopsis thaliana. Environ. Sci. Technol. 49 (2), 1113–1119.
Konate, A., Wang, Y., He, X., Adeel, M., Zhang, P., Ma, Y., Ding, Y., Zhang, J., Yang, J., Kizito, S., Rui, Y., Zhang, Z., 2018. Comparative effects of nano and bulk-Fe_3O_4 on the growth of cucumber (*Cucumis sativus*). Ecotoxicol. Environ. Saf. 165, 547–554.
Le Van, N., Ma, C., Rui, Y., Liu, S., Li, X., Xing, B., Liu, L., 2015. Phytotoxic mechanism of nanoparticles: destruction of chloroplasts and vascular bundles and alteration of nutrient absorption. Sci. Rep. 5, 116–118.
Li, J., Chang, P.R., Huang, J., Wang, Y., Yuan, H., Ren, H., 2013. Physiological effects of magnetic iron oxide nanoparticles towards watermelon. J. Nanosci. Nanotechnol. 13 (8), 5561–5567.
Li, J., Hu, J., Ma, C., Wang, Y., Wu, C., Huang, J., Xing, B., 2016. Uptake, translocation and physiological effects of magnetic iron oxide (γ-Fe_2O_3) nanoparticles in corn (*Zea mays* L.). Chemosphere 159, 326–334.
Li, J., Hu, J., Xiao, L., Wang, Y., Wang, X., 2018. Interaction mechanisms between αFe_2O_3, γ-Fe_2O_3 and Fe_3O_4 nanoparticles and *Citrus maxima* seedlings. Sci. Total Environ. 625, 677–685.
Li, X., Yang, Y., Gao, B., Zhang, M., 2015. Stimulation of peanut seedling development and growth by zerovalent iron nanoparticles at low concentrations. PLoS One 10, e0122884.
López-Moreno, M.L., de la Rosa, G., Hernández-Viezcas, J.A., Castillo-Michel, H., Botez, C.E., Peralta-Videa, J.R., Gardea-Torresdey, J.L., 2010. Evidence of the differential biotransformation and genotoxicity of ZnO and CeO_2 nanoparticles on soybean (*Glycine max*) plants. Environ. Sci. Technol. 44, 7315–7320.
Ma, X., Gurung, A., Deng, Y., 2013. Phytotoxicity and uptake of nanoscale zerovalent iron (nZVI) by two plant species. Sci. Total Environ. 443, 844–849.
Maehly, A.C., Chance, B., 1954. The assay of catalase and peroxidasa. Methods Biochem. Anal. 1, 357–424.
Marslin, G., Sheeba, C.J., Franklin, G., 2017. Nanoparticles alter secondary metabolism in plants via ROS burst. Front. Plant Sci. 8, 832.
Maswada, H.F., Djanaguiraman, M., Prasad, P.V.V., 2018. Seed treatment with nano-iron (III) oxide enhances germination, seeding growth and salinity tolerance of sorghum. J. Agron. Crop Sci. 204 (6), 577–587.
Mazaheri-Tirani, M., Dayani, S., 2020. In vitro effect of zinc oxide nanoparticles on *Nicotiana tabacum* callus compared to ZnO micro particles and zinc sulfate ($ZnSO_4$). Plant Cell Tissue Organ Cult. 140, 279–289.
Miller, G.W., Jen Huang, I., Welkie, G.W., Pushnik, J.C., 1995. Function of iron in plants with special emphasis on chloroplasts and photosynthetic activity. In: Abadía, J. (Ed.), Iron Nutrition in Soils and Plants. Developments in Plant and Soil Sciences. Springer, Dordrecht, pp. 19–28.
Mur, M., Ponce, M., Vázquez, J.M., Guilino, F., Merani, V., Palancar, T., Balbuena, R.H., 2018. Aplicación de agroquímicos en cultivos de soja (Glycine max L. Merr). Evaluación del efecto de diferentes técnicas sobre la eficiencia de distribución. Rev. Fac. Agron. 117, 77–88.
Nair, P.M., Chung, I.M., 2014. A mechanistic study on the toxic effect of copper oxide nanoparticles in soybean (*Glycine max* L.) root development and lignification of root cells. Biol. Trace Elem. Res. 162, 342–352.
Nakano, Y., Asada, K., 1981. Hydrogen peroxide is scavenged by ascorbate-specific peroxidase in spinach chloroplast. Plant Cell Physiol. 22, 867–880.
Ngan, H.T.M., Tung, H.T., Lea, B.V., Nhut, D.T., 2020. Evaluation of root growth, antioxidant enzyme activity and mineral absorbability of carnation (Dianthus caryophyllus "Express golem") plantlets cultured in two culture systems supplemented with iron nanoparticles. Sci. Hortic. 272, 109612.
Palmqvist, N.M., Seisenbaeva, G.A., Svedlindh, P., Kessler, V.G., 2017. Maghemite nanoparticles acts as nanozymes, improving growth and abiotic stress tolerance in *Brassica napus*. Nanoscale Res. Lett. 12 (1), 631.
Pariona, N., Martinez, A.I., Hdz-García, H.M., Cruz, L.A., Hernandez-Valdes, A., 2017. Effects of hematite and ferrihydrite nanoparticles on germination and growth of maize seedlings. Saudi J. Biol. Sci. 24, 1547–1554.
Rajput, V., Minkina, T., Mazarji, M., Shende, S., Sushkova, S., Saglar, M., Mandzhieva, S., Burachevskaya, M., Chaplygin, V., Singh, A., Jatav, H., 2020. Accumulation of nanoparticles in the soil-plant systems and their effects on human health. Ann. Agric. Sci. 65, 137–143.
Raliya, R., Tarafdar, J.C., 2013. ZnO nanoparticle biosynthesis and its effect on phosphorous-mobilizing enzyme secretion and gum contents in Clusterbean (*Cyamopsis tetragonoloba* L.). Agric. Res. 2, 48–57.
Rao, S., Shekhawat, G.S., 2016. Phytotoxicity and oxidative stress perspective of two selected nanoparticles in *Brassica juncea*. 3 Biotech 6 (2), 244.
Rico, C.M., Majumdar, S., Duarte-Gardea, M., Peralta-Videa, J.R., Gardea-Torresdey, J.L., 2011. Interaction of nanoparticles with edible plants and their possible implications in the food chain. J. Agric. Food Chem. 59, 3485–3498.
Rizwan, M., Ali, S., Ali, B., Adrees, M., Arshad, M., Hussain, A., Zia ur Rehman, M., Waris, A.A., 2019. Zinc and iron oxide nanoparticles improved the plant growth and reduced the oxidative stress and cadmium concentration in wheat. Chemosphere 214, 269–277.
Rui, M., Ma, C., Hao, Y., Guo, J., Rui, Y., Tang, X., Zhao, Q., Fan, X., Zhang, Z., Hou, T., 2016. Iron oxide nanoparticles as a potential iron fertilizer for peanut (*Arachis hypogaea*). Front. Plant Sci. 7, 815.
Servin, A., Elmer, W., Mukherjee, A., De la Torre-Roche, R., Hamdi, H., White, J.C., Bindraban, P., Dimkpa, C., 2015. A review of the use of engineered nanomaterials to suppress plant disease and enhance crop yield. J. Nanopart. Res. 17 (2), 1–21.
Shankramma, K., Yallappa, S., Shivanna, M.B., Manjanna, J., 2016. Fe_2O_3 magnetic nanoparticles to enhance *S. lycopersicum* (tomato) plant growth and their biomineralization. Appl. Nanosci. 6, 983–990.
Sheng-Nan, S., Chao, W., Zan-Zan, Z., Yang-Long, H., Venkatramana, S.S., Zhi-Chuan, X., 2014. Magnetic iron oxide nanoparticles: synthesis and surface coating techniques for biomedical applications. Chin. Phys. B 23 (3), 037503.
Shou, H., Bordallo, P., Fan, J.B., Yeakley, J.M., Bibikova, M., Sheen, J., Wang, K., 2004. Expression of an active tobacco mitogen-activated protein kinase enhances freezing tolerance in transgenic maize. Proc. Natl. Acad. Sci. USA 101, 3298–3303.
Sun, H., 2019. Grand challenges in environmental nanotechnology. Front. Nanotechnol. 1, 2. https://doi.org/10.3389/fnano.
Sun, Y., Jing, R., Zheng, F., Zhang, S., Jiao, W., Wang, F., 2019. Evaluating phytotoxicity of bare and starch-stabilized zerovalent iron nanoparticles in mung bean. Chemosphere 236, 124336.
Thordal-Christensen, H., Zhang, Z., Wei, Y., Collinge, D.B., 1997. Subcellular localization of H_2O_2 in plants, H_2O_2 accumulation in papillae and hypersensitive response during the barley-powdery mildew interaction. Plant J. 11, 1187–1194.
Tombuloglu, H., Slimani, Y., Tombuloglu, G., Almessiere, M., Baykal, A., 2019a. Uptake and translocation of magnetite (Fe_3O_4) nanoparticles and its impact on photosynthetic genes in barley (*Hordeum vulgare* L.). Chemosphere 226, 110–122.
Tombuloglu, H., Slimani, Y., Tombuloglu, G., Korkmaz, A.D., Baykal, A., Almessiere, M., Ercan, I., 2019b. Impact of superparamagnetic iron oxide nanoparticles (SPIONs) and ionic iron on physiology of summer squash (*Cucurbita pepo*): a comparative study. Plant Physiol. Biochem. 139, 10.1016/j.plaphy.2019.03.011.
Tripathi, D.K., Tripathi, A., Shweta Singh, S., Singh, Y., Vishwakarma, K., Yadav, G., Sharma, S., Singh, V.K., Mishra, R.K., Upadhyay, R.G., Dubey, N.K., 2017. Uptake, accumulation and toxicity of silver nanoparticle in autotrophic plants, and heterotrophic microbes: a concentric review. Front. Microbiol. 08, 07.
Trujillo-Reyes, J., Vilchis-Nestor, A.R., Majumdar, S., Peralta-Videa, J.R., Gardea-Torresdey, J.L., 2013. Citric acid modifies surface properties of commercial CeO_2 nanoparticles reducing their toxicity and cerium uptake in radish (*Raphanus sativus*) seedlings. J. Hazard. Mater. 263 (2), 677–684.
Vanková, R., Landa, P., Podlipná, R., Dobrev, P.I., Prerostova, S., Langhansova, L., Gaudinova, A., Motkova, K., Knirsch, V., Vanek, T., 2017. ZnO nanoparticle effects on hormonal pools in *Arabidopsis thaliana*. Sci. Total Environ. 593–594, 535–542.
Venkatachalam, P., Priyanka, N., Manikandan, K., Ganeshbabu, I., Indiraarulselvi, P., Geetha, N., Muralikrishna, K., Bhattacharya, R., Tiwari, M., Sharma, N., Sahi, S.V., 2017. Enhanced plant growth promoting role of phycomolecules coated zinc oxide nanoparticles with P supplementation in cotton (Gossypium hirsutum L.). Plant Physiol. Biochem. 110, 118–127.
Wang, H., Kou, X., Pei, Z., Xiao, J.Q., Shan, X., Xing, B., 2011. Physiological effects of magnetite (Fe_3O_4) nanoparticles on perennial ryegrass (*Lolium perenne* L.) and pumpkin (*Cucurbita mixta*) plants. Nanotoxicology 5, 30–42.
Wang, J., Fang, Z., Cheng, W., Yan, X., Tsang, P.E., Zhao, D., 2016. Higher concentrations of nanoscale zerovalent iron (nZVI) in soil induced rice chlorosis due to inhibited active iron transportation. Environ. Pollut. 210, 338–345.
Wintermans, J.F., de Mots, A., 1965. Spectrophotometric characteristics of chlorophylls a and b and their pheophytins in ethanol. Biochim. Biophys. Acta 109, 448–453.
Wu, W., He, Q., Jiang, C., 2008. Magnetic iron oxide nanoparticles: synthesis and surface functionalization strategies. Nanoscale Res. Lett. 3, 397–415.

Xia, T., Wang, J., Wu, C., Meng, F., Shi, Z., Lian, J., Feng, J., Meng, J., 2012. Novel complex-coprecipitation route to form high quality triethanolamine-coated Fe_3O_4 nanocrystals: their high saturation magnetizations and excellent water treatment properties. CrystEngComm 14, 5741–5744.

Yan, L., Li, P., Zhao, X., Ji, R., Zhao, L., 2020. Physiological and metabolic responses of maize (*Zea mays*) plants to Fe_3O_4 nanoparticles. Sci. Total Environ. 718, 137400.

Yanık, F., Vardar, F., 2018. Oxidative stress response to aluminum oxide (Al_2O_3) nanoparticles in *Triticum aestivum*. Biologia 73, 129–135.

Yasmeen, F., Razzaq, A., Iqbal, M.N., Jhanzab, H.M., 2015. Effect of silver, copper and iron nanoparticles on wheat germination. Int. J. Biosci. 6, 112–117.

Yuan, J., Chen, Y., Li, H., Lu, J., Zhao, H., Liu, M., Nechitaylo, G.S., Glushchenko, N.N., 2018. New insights into the cellular responses to iron nanoparticles in *Capsicum annuum*. Sci. Rep. 8, 3228.

Zhai, G., Walters, K.S., Peate, D.W., Alvarez, P.J., Schnoor, J.L., 2014. Transport of gold nanoparticles through plasmodesmata and precipitation of gold ions in woody poplar. Environ. Sci. Technol. Lett. 1, 146–151.

Zhao, L., Peng, B., Hernandez-Viezcas, J.A., Rico, C., Sun, Y., Peralta-Videa, J.R., Tang, X., Niu, G., Jin, L., Varela-Ramirez, A., Zhang, J.Y., Gardea-Torresdey, J.L., 2012. Stress response and tolerance of Zea mays to CeO_2 nanoparticles: cross talk among H_2O_2, heat shock protein, and lipid peroxidation. ACS Nano 6, 9615–9622.

Zhu, H., Han, J., Xiao, J.Q., Jin, Y., 2008. Uptake, translocation, and accumulation of manufactured iron oxide nanoparticles by pumpkin plants. J. Environ. Monit. 10, 713–717.

Zhu, Z.J., Wang, H., Yan, B., Zheng, H., Jiang, Y., Miranda, O.R., Rotello, V.M., Xing, B., Vachet, R.W., 2012. Effect of surface charge on the uptake and distribution of gold nanoparticles in four plant species. Environ. Sci. Technol. 46, 12391–12398.